

Far-infrared absorption by shallow donors in multiple-well GaAs-Ga_{1-x}Al_xAs heterostructures

Ronald L. Greene and Pat Lane

Department of Physics, University of New Orleans, New Orleans, Louisiana 70148

(Received 28 May 1986)

We report the results of calculations of multiple-well effects upon the energies of shallow donors and their influence upon far-infrared absorption profiles. We have calculated the binding energies of the ground and first few excited states for a variety of well and barrier widths and magnetic field strengths. For a uniform donor distribution the profiles show several peaks, the strongest corresponding to transitions to excited states of donors located near the center of a barrier. Significantly weaker peaks occur which correspond to similar transitions for donors located near the center of a well.

I. INTRODUCTION

In 1983 Bastard *et al.*¹ reported calculations of the expected absorption profile for transitions from the ground to the $2p_{\pm}$ -like excited states of shallow donors distributed uniformly in a single GaAs well bounded by infinitely high barriers. The variation of the transition energy with donor position causes the ordinarily sharp line to broaden, with a peak for donors located at or near the center of the well. Later Greene and Bajaj² performed similar calculations with several extensions. First, they assumed a more realistic, finite height for the Ga_{1-x}Al_xAs barriers on either side of the single well. In addition, they included effects due to donors located in both the barrier and the well materials. Finally, they considered the case of a uniform magnetic field aligned with the growth axis, perpendicular to the interfaces between the well and barriers. Early comparisons with experimental profiles from heterostructures doped with donors near the centers of the wells were favorable.³

We have extended the work of Greene and Bajaj by incorporating often significant effects due to the finite widths of Ga_{1-x}Al_xAs barrier regions between GaAs wells, and including transitions to $3p_{\pm}$ -like states in the absorption calculations.

II. THEORY

A. Variational wave functions

The effective-mass Hamiltonian for a shallow donor in a heterostructure with a uniform magnetic field applied perpendicular to the layers is given by⁴

$$H = -\nabla^2 - 2/r + \gamma L_z + \gamma^2 \rho^2 / 4 + V_w(z). \quad (1)$$

This equation has been expressed in dimensionless form. The unit of energy is the bulk GaAs effective rydberg ($R^* = 5.83$ meV), and the unit of length is the effective Bohr radius in GaAs ($a_0^* = 98.7$ Å). The electron's position relative to the impurity is given by $r = [\rho^2 + (z - z_I)^2]^{1/2}$, where ρ is the distance in the x - y plane and z_I is the position of the impurity atom. The

quantity γ is a dimensionless measure of the magnetic field, defined as

$$\gamma = e\hbar B / (2m^* c R^*). \quad (2)$$

In this equation m^* is the effective mass of the electron in the heterostructure, which we assume to be the same as in bulk GaAs.

To simulate the effects of multiple wells, we take $V_w(z)$ to be a periodic one-dimensional square-well potential. The model is discussed in Ref. 5.

We have used variational wave functions of the basic forms given in Refs. 4 and 5. Briefly, we write the variational wave function as

$$\Psi(\rho, z, \phi) = f(z) G(\rho, z - z_I, \phi), \quad (3)$$

where $f(z)$ is the lowest energy solution to the periodic square-well problem.⁵ The function $G(\rho, z - z_I)$ is assumed to depend only on electron-impurity relative coordinates,⁴

$$G(\rho, z - z_I, \phi) = \rho^{|m|} e^{im\phi} \sum_{i,j} A_{ij} G_{ij}(\rho, z - z_I). \quad (4)$$

The cylindrical symmetry ensures that the component of angular momentum along the z axis is conserved; m is the quantum number associated with this angular momentum. The basis functions $G_{ij}(\rho, z - z_I)$ are Gaussians,

$$G_{ij}(\rho, z) = \exp[-(\alpha_i + \beta)\rho^2 - \alpha_j z^2]. \quad (5)$$

The quantity β is a parameter, proportional to γ , which provides for the constriction of the wave function by the magnetic field. We used $\beta = 0.1\gamma$ for most cases, although the energies are not very sensitive to the proportionality constant. The parameters α_i were taken from the results of Huzinaga⁶ who did a detailed study of the use of Gaussian basis functions in the calculations of hydrogen atom energy levels. We extended the set of α_i beyond that of Refs. 4 and 5 to accurately account for the influence of $n = 3$ like levels upon the absorption profiles. The α_i set (13.4, 2.01, 0.454, 0.123, 0.0324, 0.00717) was used in 16 basis functions for our final calculations.

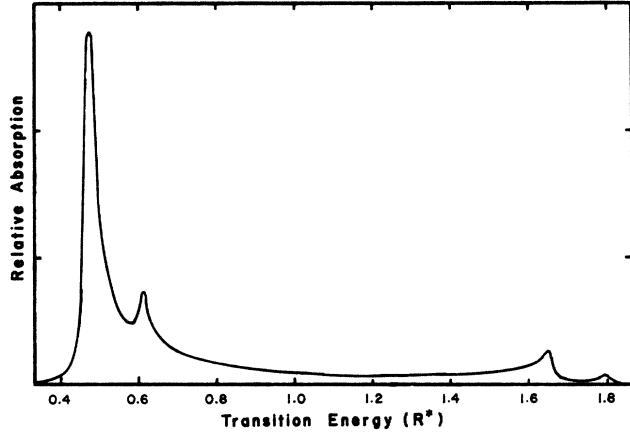


FIG. 1. Relative absorption as a function of energy for a uniform impurity distribution. The well and barrier widths are 100 Å, and the magnetic field parameter $\gamma=0$. The aluminum fraction is $x=0.3$.

B. Absorption profiles

The theory of absorption of light by shallow donors in quantum-well heterostructures is summarized in Ref. 2. We seek to calculate the line-shape function for absorption of light polarized in x direction (parallel to heterostructure interfaces),

$$I(\omega) = \omega \sum_f \int_{-\infty}^{\infty} dz_I \lambda(z_I) |\langle f | x | i \rangle|^2 \delta(\omega - E_{fi}/\hbar). \quad (6)$$

In this expression $\lambda(z_I)$ is the linear density of donor impurities in the heterostructure, and E_{fi} is the transition energy from initial state $|i\rangle$ to final state $|f\rangle$. Note that the transition energies and the states $|i\rangle$ and $|f\rangle$ depend on z_I .

The initial (ground) states are states of zero angular momentum projection along the z axis ($m=0$ states). Thus the matrix elements of the x operator vanish for all final states except those for which $m=\pm 1$. In addition, we assume that the frequency of incident radiation is such that only the two lowest states for each m value contribute to $I(\omega)$ in the region of interest. The sum over final states is then reduced to a few terms.

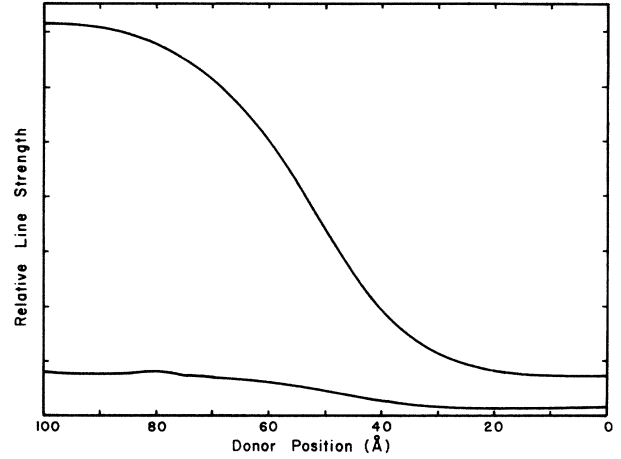


FIG. 2. Line strength ($|\langle f | x | i \rangle|^2$) as a function of donor position. The conditions are the same as for Fig. 1. The upper curve corresponds to the ground to first $m=\pm 1$ states, and the lower curve corresponds to the ground to second $m=\pm 1$ states. The donor position is measured from the center of a well, so that 100 Å is at the center of a barrier, and 50 Å is at the interface between semiconductors.

For the results presented in Sec. III we replaced the δ functions in Eq. (6) with narrow Lorentzians,

$$\delta(\omega) \simeq (\Gamma/\pi)(\omega^2 + \Gamma^2)^{-1}. \quad (7)$$

This is a numerical approximation, although it could be used empirically to approximate the effects of other broadening mechanisms that have been neglected in obtaining the expression for $I(\omega)$. We chose the width Γ to be sufficiently small that it has very little effect upon the final profile. This was checked by comparison of results with successively smaller values for Γ .

III. RESULTS AND DISCUSSION

We have performed calculations of the line-shape function $I(\omega)$ for a uniform distribution of donors and for various combinations of well width ($50 < L < 150$ Å), barrier width ($50 < b < 300$ Å), and magnetic field strength ($0.0 < \gamma < 1.0$). All cases have several features in common. For $\gamma=0.0$, each profile shows a set of two peaks for the lowest energy $m=0$ to $m=\pm 1$ transitions at the

TABLE I. Transition energies for donors located at the center of a barrier (Δ_{1b} and Δ_{2b}), center of a well (Δ_{1w} and Δ_{2w}), and the interface (Δ_{1i}). The magnetic field strength is $\gamma=0.0$. Energies are in GaAs effective rydbergs (5.83 meV).

L (Å)	b (Å)	Δ_{1b}	Δ_{2b}	Δ_{1w}	Δ_{2w}	Δ_{1i}
50	50	0.64	0.78	1.07	1.21	0.74
50	100	0.59	0.73	1.92	2.07	1.06
100	50	0.58	0.72	1.42	1.56	0.63
100	100	0.47	0.61	1.66	1.81	0.68
100	200	0.37	0.51	1.73	1.96	1.01
150	150	0.37	0.51	1.53	1.74	0.61
150	300	0.23	0.36	1.50	1.76	0.74

TABLE II. Transition energies for donors located at the center of a barrier (Δ_{1b} and Δ_{2b}), center of a well (Δ_{1w} and Δ_{2w}), and the interface (Δ_{1i}). The magnetic field strength is $\gamma=0.2$. Energies are in GaAs effective rydbergs.

L (Å)	b (Å)	Δ_{1b}	Δ_{2b}	Δ_{1w}	Δ_{2w}	Δ_{1i}
50	50	0.57	0.89	1.01	1.33	0.67
50	100	0.51	0.83	1.85	2.18	0.99
100	50	0.50	0.82	1.35	1.68	0.55
100	100	0.39	0.70	1.57	1.88	0.60
100	200	0.27	0.56	1.62	1.99	0.91
150	150	0.28	0.57	1.42	1.77	0.53
150	300	0.15	0.42	1.39	1.80	0.64

TABLE III. Transition energies for donors located at the center of a barrier (Δ_{1b} and Δ_{2b}), center of a well (Δ_{1w} and Δ_{2w}), and the interface (Δ_{1i}). The magnetic field strength is $\gamma=0.4$. Energies are in GaAs effective rydbergs.

L (Å)	b (Å)	Δ_{1b}	Δ_{2b}	Δ_{1w}	Δ_{2w}	Δ_{1i}
50	50	0.57	1.00	1.03	1.48	0.68
50	100	0.49	0.92	1.86	2.30	1.01
100	50	0.49	0.92	1.37	1.82	0.55
100	100	0.37	0.78	1.57	1.95	0.61
100	200	0.24	0.60	1.58	2.10	0.88
150	150	0.24	0.62	1.38	1.82	0.53
150	300	0.13	0.48	1.36	1.93	0.61

TABLE IV. Transition energies for donors located at the center of a barrier (Δ_{1b} and Δ_{2b}), center of a well (Δ_{1w} and Δ_{2w}), and the interface (Δ_{1i}). The magnetic field strength is $\gamma=0.6$. Energies are in GaAs effective rydbergs.

L (Å)	b (Å)	Δ_{1b}	Δ_{2b}	Δ_{1w}	Δ_{2w}	Δ_{1i}
50	50	0.57	1.12	1.07	1.61	0.69
50	100	0.49	0.99	1.88	2.39	1.04
100	50	0.49	1.02	1.41	1.95	0.55
100	100	0.35	0.85	1.57	2.03	0.62
100	200	0.21	0.63	1.57	2.21	0.87
150	150	0.22	0.65	1.37	1.99	0.53
150	300	0.11	0.51	1.35	2.06	0.60

TABLE V. Transition energies for donors located at the center of a barrier (Δ_{1b} and Δ_{2b}), center of a well (Δ_{1w} and Δ_{2w}), and the interface (Δ_{1i}). The magnetic field strength is $\gamma=0.8$. Energies are in GaAs effective rydbergs.

L (Å)	b (Å)	Δ_{1b}	Δ_{2b}	Δ_{1w}	Δ_{2w}	Δ_{1i}
50	50	0.58	0.82	1.12	1.73	0.72
50	100	0.48	1.06	1.90	2.48	1.08
100	50	0.49	1.09	1.44	2.06	0.56
100	100	0.33	0.91	1.59	2.13	0.63
100	200	0.20	0.66	1.58	2.34	0.86
150	150	0.21	0.68	1.37	2.10	0.54
150	300	0.10	0.58	1.36	2.19	0.59

TABLE VI. Transition energies for donors located at the center of a barrier (Δ_{1b} and Δ_{2b}), center of a well (Δ_{1w} and Δ_{2w}), and the interface (Δ_{1i}). The magnetic field strength is $\gamma=1.0$. Energies are in GaAs effective rydbergs.

L (Å)	b (Å)	Δ_{1b}	Δ_{2b}	Δ_{1w}	Δ_{2w}	Δ_{1i}
50	50	0.59	1.28	1.16	1.85	0.74
50	100	0.48	1.11	1.93	2.53	1.12
100	50	0.49	1.15	1.48	2.17	0.57
100	100	0.33	0.97	1.61	2.23	0.64
100	200	0.19	0.70	1.59	2.45	0.86
150	150	0.20	0.72	1.38	2.21	0.54
150	300	0.09	0.67	1.37	2.31	0.59

energies corresponding to donors located at the center of a well and the center of a barrier. These occur because of the large density of states associated with these energies.² For $\gamma > 0.0$, each of these peaks splits into two, separated by 2γ . The peak(s) associated with donors at the center of a barrier is (are) significantly stronger than that (those) for donors at the center of a well.

A weaker set of peaks occurs which corresponds to the ground to second $m = \pm 1$ excited states ($3p_{\pm}$ like). For most cases these peaks do not rise very much above the general background, due to small dipole matrix elements. Transitions to still higher excited states neglected in our calculations may cause these peaks to degenerate into plateaulike structures near these energies rather than distinct peaks.

Figure 1 shows a typical zero-field absorption profile. The case shown is one in which the well and barrier widths are 100 Å. The largest effect of varying these widths is to vary the spacing between the set of higher- and lower-energy peaks. This can be seen in the accompanying tables. As mentioned above, the major visual effect of applying a magnetic field is to cause each of the peaks of Fig. 1 to split by 2γ .

The primary reason that the low-energy peaks are stronger than the high-energy peaks is that the line strength for a donor at the center of a barrier is significantly larger than it is when the donor is at the center of a well. This is true for both sets of $m = \pm 1$ excited states, as shown in Fig. 2. In that figure the curve with the larger line strength corresponds to the first $m = \pm 1$ excited states ($2p_{\pm}$ like), while the lower-strength curve applies to higher-energy $m = \pm 1$ states ($3p_{\pm}$ like). The slight ripple in the lower curve at about 80 Å is probably a calculational artifact, since our variational wave functions for the higher-excited states are not quite as accurate as for the first excited-state set.

As noted earlier, Fig. 1 applies to the case of a uniform impurity distribution. Cases in which the impurities are intentionally doped in the GaAs only or in the $\text{Ga}_{1-x}\text{Al}_x\text{As}$ only can be easily obtained from this figure by respectively zeroing the contribution to the absorption for energies less than or greater than the transition energy for a donor at the interface. This energy can be found in the tables.

In Tables I–VI we present the $m = 0$ to $m = -1$ tran-

sition energies of donors located at the centers of a barrier or well for a variety of L , b , and γ values. The aluminum fraction is $x = 0.3$, and the barrier height is $0.6\Delta E_g$, where ΔE_g is the band-gap difference between $\text{Ga}_{1-x}\text{Al}_x\text{As}$ and GaAs, given by $\Delta E_g = (1.155x + 0.37x^2)$ eV.⁷ The symbol Δ_{1b} (Δ_{1w}) represents the transition energy for ground to first $m = -1$ excited state for a donor at the center of a barrier (well). The symbol Δ_{2b} (Δ_{2w}) represents the similar transition from ground to second $m = -1$ excited state. For $\gamma > 0$ the $m = +1$ energies will be shifted by 2γ from the values shown in the tables. In all cases strong peaks occur at energies very near Δ_{1b} , and significantly weaker, but distinct peaks occur near Δ_{1w} for uniformly distributed donors.

Also shown in Tables I–VI are the energies for the lowest $m = 0$ to $m = -1$ transition for donors located at an interface between GaAs and $\text{Ga}_{1-x}\text{Al}_x\text{As}$. This column is labeled Δ_{1i} . Although there is no peak associated with this location for a uniform donor distribution, there is some evidence to suggest that impurities may accumulate at the interfaces between semiconductors. Such an accumulation would produce a local peak in $\lambda(z_I)$ of Eq. (6), and a corresponding peak in the absorption spectrum.

The experimental situation is still not completely clear. Jarosik *et al.*³ have reported good agreement between their far-infrared magnetospectroscopy data and the single-well results of Greene and Bajaj² for the donor at the center of the well. Our present calculations should also be in good agreement since the multiple-well effects are not very important for such donors in moderate to large wells and barriers ($L, b > a_0^*$). These experiments used GaAs- $\text{Ga}_{1-x}\text{Al}_x\text{As}$ samples doped with donors at or near the center of the GaAs wells, so that it is unlikely that they would have seen a spectral feature associated with donors in a barrier. Similar experiments with doped $\text{Ga}_{1-x}\text{Al}_x\text{As}$ layers should be of interest in an experimental study of confinement effects.

ACKNOWLEDGMENT

This work was partially supported by Southeastern Center for Electrical Engineering Education Subcontract No. 84-RIP-17 and by the University of New Orleans Research Council.

¹G. Bastard, E. E. Mendez, L. L. Chang, and L. Esaki, *Solid State Commun.* **45**, 367 (1983).

²Ronald L. Greene and K. K. Bajaj, *Phys. Rev. B* **34**, 951 (1986).

³N. C. Jarosik, B. D. McCombe, B. V. Shanabrook, J. Comas, John Ralston, and G. Wicks, *Phys. Rev. Lett.* **54**, 1283 (1985).

⁴Ronald L. Greene and K. K. Bajaj, *Phys. Rev. B* **31**, 913 (1985).

⁵Pat Lane and Ronald L. Greene, *Phys. Rev. B* **33**, 5871 (1986).

⁶S. Huzinaga, *J. Chem. Phys.* **42**, 1293 (1965).

⁷H. J. Lee, L. Y. Juravel, J. C. Woolley, and A. J. Springthorpe, *Phys. Rev. B* **21**, 659 (1980).